

Constant surface gravity and density profile of dark matter

H. J. de Vega*

*LPTHE, Laboratoire Associé au CNRS UMR 7589,
Université Pierre et Marie Curie (Paris VI) et Denis Diderot (Paris VII),
Tour 24, 5 ème. étage, 4, Place Jussieu, 75252 Paris, Cedex 05,
France and Observatoire de Paris, LERMA, Laboratoire Associé au CNRS UMR 8112,
61, Avenue de l'Observatoire, 75014 Paris, France.*

N. G. Sanchez†

*Observatoire de Paris, LERMA, Laboratoire Associé au CNRS UMR 8112,
61, Avenue de l'Observatoire, 75014 Paris, France.*

Cumulative observational evidence confirm that the surface gravity of dark matter (DM) halos $\mu_{0D} = r_0 \rho_0$ where r_0 and ρ_0 are the halo core radius and central density, respectively, is nearly **constant** and independent of galaxy luminosity for a high number of galactic systems (spirals, dwarf irregular and spheroidals, elliptics) spanning over 14 magnitudes in luminosity and of different Hubble types. Remarkably, its numerical value $\mu_{0D} \simeq 140 M_\odot/\text{pc}^2 = (18.6 \text{ MeV})^3$ is approximately **the same** (up to a factor of two) in all these systems. First, we present the physical consequences of the independence of μ_{0D} on r_0 : the energy scales as the volume $\sim r_0^3$ while the mass and the entropy scale as the surface $\sim r_0^2$ and the surface times $\log r_0$, respectively. Namely, the entropy scales similarly to the black-hole entropy but with a much smaller coefficient. Second, we compute the surface gravity and the density profile for small scales from first principles and the evolution of primordial density fluctuations since the end of inflation till today using the linearized Boltzmann-Vlasov equation. The density profile $\rho_{lin}(r)$ obtained in this way decreases as $r^{-1-n_s/2}$ for intermediate scales where $n_s \simeq 0.964$ is the **primordial** spectral index. This scaling is in remarkable agreement with the empirical behaviour found observationally and in N -body simulations: $r^{-1.6 \pm 0.4}$. The observed value of μ_{0D} indicates that the DM particle mass m is in the keV scale. The theoretically derived density profiles $\rho_{lin}(r)$ turn to be **cored** for m in the keV scale and they look as **cusped** for m in the GeV scale or beyond. We consider both fermions and bosons as DM particles decoupling either ultrarelativistically or non-relativistically. Our results do **not** use any particle physics model and vary slightly with the statistics of the DM particle.

Contents

I. Observational evidences	1
II. Constant surface gravity and the scaling of the mass, energy and entropy	2
III. The density profile and the surface gravity from the linearized Boltzmann-Vlasov equation	4
IV. Properties of the linear density profile and the surface gravity	7
V. Concluding remarks and the DM particle mass in the keV scale	9
Acknowledgments	11
References	11

I. OBSERVATIONAL EVIDENCES

Growing recent findings point towards a constant dark matter (DM) surface gravity μ_{0D} in galaxy DM halos [16, 28, 41]. Namely, the product $\mu_{0D} \equiv r_0 \rho_0$ where r_0 and ρ_0 are the halo core radius and central density, respectively, is nearly **constant**, over a large number of galaxies of different kinds

$$\mu_{0D} \simeq 140 \frac{M_\odot}{\text{pc}^2} = 6400 \text{ MeV}^3 = (18.6 \text{ MeV})^3, \quad (1.1)$$

*Electronic address: devega@lpthe.jussieu.fr

†Electronic address: Norma.Sanchez@obspm.fr

while r_0 varies by two orders of magnitude [16, 28, 41]:

$$0.3 \text{ kpc} < r_0 < 30 \text{ kpc} \quad \text{and} \quad 10^{-25} \text{ g/cm}^3 \leq \rho_0 \leq 6 \times 10^{-23} \text{ g/cm}^3 . \quad (1.2)$$

This finding relates to data sets (high quality rotation curves, kinematics, galaxy-galaxy weak lensing signals) for many galactic systems spanning over 14 magnitudes in luminosity and of different Hubble type, dwarf disk and spheroidals, spirals, ellipticals. In spite of their different properties, μ_{0D} in galaxies is essentially **independent** of their luminosity and mass. The surface gravity μ_{0D} is also the surface density.

For luminous matter, the surface gravity takes also the value eq.(1.1) provided μ_{0D} is obtained as the product of the halo core radius r_0 times the density at r_0 [18].

It must be noticed that relations analogous to the eq.(1.1) are also known for interstellar molecular clouds in our Galaxy [32]. One of the scaling laws put forward by Larson [32] states that the surface gravity (column density) μ_{0D} is approximately a **constant** over more than four orders of magnitude of scales $0.001 \text{ pc} < r_0 < 100 \text{ pc}$. The values given in Larson [32] are:

$$\mu_{0D} = 10.5 \cdot 10^{21} \frac{m_{H_2}}{\text{cm}^2} = 162 \frac{M_\odot}{\text{pc}^2}$$

where m_{H_2} stands for the mass of the Hydrogen molecule, main constituent of the interstellar clouds. Recent data averaged over high density regions of Taurus give [22]

$$\mu_{0D} = 5.14 \cdot 10^{21} \frac{m_{H_2}}{\text{cm}^2} = 80 \frac{M_\odot}{\text{pc}^2} \quad (1.3)$$

The mean density of structures in the ISM vary between 10 and 10^5 atoms/cm³, significantly above the mean ISM density which is about 0.1 atoms/cm³ or $1.6 \cdot 10^{-25}$ g/cm³. Hence eqs.(1.1) and (1.3) are verified both for molecular clouds and galaxies (up to a factor 2).

The quantities r_0 and ρ_0 depend on the particular galaxy (or molecular cloud) chosen and are therefore functions of the past history of the galaxy (or cloud). Instead, the product $\mu_{0D} = r_0 \rho_0$ given by eq.(1.1) is an **universal** number for all galactic systems and molecular clouds and hence independent of the previous history of the system. Therefore, μ_{0D} can only depend on **universal quantities**. Since μ_{0D} is the same (up to a factor two) for molecular clouds and galaxies, the action of self-gravity (both of baryonic and dark matter) should be responsible of its value since it is the only common physical mechanism to all these objects. Indeed, other processes play a role in the physics of molecular clouds and galaxies and can affect the surface gravity deviating it from the universal value eq.(1.1) by a factor of two or so (see for example Heyer et al. [23]). These processes are therefore **subdominant** with respect to self-gravity. For example, the observed mean surface gravity in the M64 galaxy is $10^{22} m_{H_2}/\text{cm}^2$ [37] within 15 % of our equation (1.1).

As stressed in Disney et al. [14], Garcia-Appadoo et al. [17], Persic et al. [34], van den Bergh [44], a single parameter should control the galaxy structure implying that functional relations must constrain galaxy parameters as mass, size, baryon-fraction, etc. We propose that the surface gravity μ_{0D} (as a function of these galaxy parameters) can be one of these functional relations necessary to explain the parameter correlations presented in Disney et al. [14], Garcia-Appadoo et al. [17], Persic et al. [34], van den Bergh [44].

This implies that μ_{0D} is independent of the baryon-fraction value. Such independence is consistent with the fact that molecular clouds (dominated by baryons) have similar μ_{0D} that DM dominated galaxies [see eqs.(1.3) and (1.1)].

We analyze in the next section how the mass, the energy and the entropy scale with the size r_0 as a consequence that μ_{0D} is a universal constant and therefore independent of r_0 in the context of kinetic theory for self-gravitating systems.

In section III we derive the value of μ_{0D} and the density profile for small scales from first principles. We use as appropriate initial conditions the primordial inflationary power spectrum and we follow the evolution through the radiation and matter dominated eras using the linearized Boltzmann-Vlasov equation for self-gravitating DM. In sections IV and V we derive the properties and implications of the obtained linear density profiles and surface gravity. The derivations presented in sections III to V do not rely on the analysis made in sec. II as they are independent of it.

II. CONSTANT SURFACE GRAVITY AND THE SCALING OF THE MASS, ENERGY AND ENTROPY

Considering that the dark matter distribution in galaxies is characterized by a scale r_0 , the matter density can be written as

$$\rho(r) = \rho_0 F\left(\frac{r}{r_0}\right) \quad , \quad F(0) = 1 . \quad (2.1)$$

Algebraic fits to the DM cored density profile [10, 41] and thermal profiles are particular examples of eq.(2.1). We have for the Burkert [10] and Spano [41] profiles (denoted F_B and F_S , respectively):

$$F_B(x) = \frac{1}{(1+x)(1+x^2)}, \quad F_S(x) = \frac{1}{(1+x^2)^{\frac{3}{2}}}, \quad x \equiv \frac{r}{r_0},$$

Notice that both the Burkert and the Spano profiles decay for large distances with the same $1/r^3$ tail as the cuspy Navarro-Frenk-White profile.

Each galaxy can be considered as an isolated system. The virial theorem for isolated self-gravitating systems (that is, zero external pressure) states that the total energy E is related to the average potential energy $\langle U \rangle$ and the average kinetic energy $\langle K \rangle$ by [29]

$$E = \frac{1}{2} \langle U \rangle = -\langle K \rangle. \quad (2.2)$$

We can therefore express the total energy E in terms of the average gravitational potential energy as

$$E = -\frac{1}{4} G \int \frac{d^3r d^3r'}{|\vec{r} - \vec{r}'|} \langle \rho(r) \rho(r') \rangle = -\frac{1}{4} G \rho_0^2 r_0^5 \int \frac{d^3x d^3x'}{|\vec{x} - \vec{x}'|} \langle F(x) F(x') \rangle. \quad (2.3)$$

Hence, since the integrals over \vec{x} and \vec{x}' in eq.(2.3) are of order one, the energy divided by the characteristic volume r_0^3 goes as

$$\frac{-E}{r_0^3} \sim G \rho_0^2 r_0^2 = G \mu_{0D}^2. \quad (2.4)$$

The mass density eq.(2.1) inserted in the Poisson equation

$$\nabla^2 \phi(r) = 4\pi G \rho(r),$$

yields a gravitational potential $\phi(r)$ of the form

$$\phi(r) = G r_0^2 \rho_0 \Phi(x), \quad (2.5)$$

where $\Phi(x)$ is a dimensionless function.

The matter density $\rho(r)$ can be expressed in the kinetic theory framework as an integral over the velocities

$$\rho(r) = m \int f(\vec{p}, \vec{r}) d^3p$$

where $f(\vec{p}, \vec{r})$ is the distribution function and m the mass of the DM particles. $f(\vec{p}, \vec{r})$ obeys the Boltzmann-Vlasov equation

$$\frac{\partial f}{\partial t} + \frac{1}{m} \vec{p} \cdot \frac{\partial f}{\partial \vec{r}} - m \frac{\partial \phi}{\partial \vec{r}} \cdot \frac{\partial f}{\partial \vec{p}} = 0 \quad (2.6)$$

and it is normalized by the total number of particles N as

$$\int f(\vec{p}, \vec{r}) d^3p d^3r = N. \quad (2.7)$$

The appropriate dimensionless variables for the Boltzmann-Vlasov equation (2.6) and the gravitational potential eq.(2.5) are defined as

$$\vec{r} = r_0 \vec{x}, \quad \vec{p} = m r_0 \sqrt{G \rho_0} \vec{q}, \quad t = \frac{\tau}{\sqrt{G \rho_0}}, \quad (2.8)$$

Here \vec{q} and τ stand for the dimensionless momentum and time, respectively. It is convenient to introduce a dimensionless distribution function

$$\mathcal{F}(\vec{q}, \vec{x}) = m^4 r_0^3 G^{\frac{3}{2}} \sqrt{\rho_0} f(\vec{p}, \vec{r}), \quad (2.9)$$

which enjoys the property,

$$\int d^3q \mathcal{F}(\vec{q}, \vec{x}) = F(x) \quad .$$

Since the integral of $F(x)$ over a volume of order one in \vec{x} is also of order one, the total mass from eq.(2.1) scales as

$$M = m N \sim r_0^3 \rho_0 = \mu_{0D} r_0^2 . \quad (2.10)$$

and

$$\int d^3q d^3x \mathcal{F}(\vec{q}, \vec{x}) = \mathcal{O}(1) \quad (2.11)$$

where $\mathcal{O}(1)$ means $\mathcal{O}([r_0]^0)$, independent of the halo size r_0 .

We can estimate the entropy

$$S = \int f(\vec{p}, \vec{r}) \log f(\vec{p}, \vec{r}) d^3p d^3r .$$

From eqs. (2.8), (2.9) and (2.11) we obtain

$$S \sim r_0^3 \frac{\rho_0}{m} \log r_0 = r_0^2 \log r_0 \frac{\mu_{0D}}{m} . \quad (2.12)$$

The average kinetic energy follows from the distribution function eq.(2.9) to be

$$K = \frac{1}{2m} \int f(\vec{p}, \vec{r}) \vec{p}^2 d^3p d^3r = \frac{1}{2} G r_0^5 \rho_0^2 \int d^3q d^3x \vec{q}^2 \mathcal{F}(\vec{q}, \vec{x}) \sim G r_0^5 \rho_0^2 = G \mu_{0D}^2 r_0^3 , \quad (2.13)$$

and similarly for the total energy eq.(2.4).

The average squared velocity

$$\langle v^2 \rangle = \frac{\langle \vec{p}^2 \rangle}{m^2}$$

follows from eq.(2.8) to be equal to

$$\langle v^2 \rangle = \frac{1}{m^2} \frac{\int \vec{p}^2 f(\vec{p}, \vec{r}) d^3p d^3r}{\int f(\vec{p}, \vec{r}) d^3p d^3r} \sim G \mu_{0D} r_0 . \quad (2.14)$$

Notice that although the above derivation applies to the DM mass distribution the results may be also true for systems where the baryonic mass is important and hence for such systems the above derivation should be generalized adding the baryonic contribution.

We thus find that a constant surface gravity μ_{0D} (that is, independent of the halo radius r_0) implies that the energy (total, potential and kinetic) scales as the volume ($\sim r_0^3$) eqs.(2.3), (2.4) and (2.13) while the total mass and entropy scale as the surface ($\sim r_0^2$) and the surface times $\log r_0$, respectively [eqs. (2.10) and (2.12)].

This scaling follows from the long range nature of the gravitational interactions plus the fact that this system is not in thermal equilibrium but in quasi-equilibrium configurations.

The **entropy** scales as the **surface** also for black-holes. However, for black-holes of mass M and area $A = 16 \pi G^2 M^2$, the entropy $S_{BH} = A/(4 G) = 4 \pi G M^2$. That is, the proportionality coefficients c between entropy and area are very different:

$$c_{gal} = \frac{S_{gal}}{r_0^2} \sim \frac{\mu_{0D}}{m} , \quad c_{BH} = \frac{S_{BH}}{A} = \frac{1}{4 G} \quad \text{which implies} \quad \frac{c_{BH}}{c_{gal}} \sim \frac{m}{\text{keV}} 10^{36}$$

showing that the entropy per unit area of the galaxy is much smaller than the entropy of a black-hole. In other words, the Bekenstein bound for the entropy of physical is well satisfied here.

Notice that the surface gravity acceleration is given by $G \mu_{0D}$.

We derive in the next section μ_{0D} as a dynamical scale determined by gravitational clustering. We consider in what follows DM in galaxies.

III. THE DENSITY PROFILE AND THE SURFACE GRAVITY FROM THE LINEARIZED BOLTZMANN-VLASOV EQUATION

The mass density $\rho_{in}(r)$ can be evaluated theoretically solving the linearized Boltzmann-Vlasov equation for self-gravitating DM in the matter dominated (MD) era. It is convenient to recast such equation as an integral equation,

namely the Gilbert equation which is a Volterra equation of second kind [5, 8, 19]. To linear order in perturbations the distribution function of the decoupled particles can be written as

$$f(\vec{x}, \vec{p}; t) = g f_0(p) + F_1(\vec{x}, \vec{p}; t)$$

where \vec{x}, \vec{p} are comoving coordinates, g is the number of internal degrees of freedom of the DM particle, typically $1 \leq g \leq 4$, $f_0(p)$ is the thermal equilibrium unperturbed distribution function at the decoupling temperature T_d normalized by

$$m g \int \frac{d^3 p}{(2\pi)^3} f_0(p) = \rho_{DM} = \Omega_M \rho_c, \quad (3.1)$$

where $\Omega_M = 0.233$ is the DM fraction, ρ_c is the critical density of the Universe

$$\rho_c = 3 M_{Pl}^2 H_0^2 = (2.518 \text{ meV})^4, \quad 1 \text{ meV} = 10^{-3} \text{ eV} \quad (3.2)$$

and $H_0 = 1.5028 \cdot 10^{-42} \text{ GeV}$. Terms of order higher than one in F_1 are neglected in the Boltzmann-Vlasov equation. The physical initial conditions at t_{eq} , the beginning of the MD era, are

$$f(\vec{x}, \vec{p}; t_{eq}) = g f_0(p)[1 + \delta(\vec{x}, t_{eq})], \quad F_1(\vec{x}, \vec{p}; t_{eq}) = g f_0(p) \delta(\vec{x}, t_{eq}), \quad (3.3)$$

where $\delta(\vec{x}, t_{eq})$ are the density fluctuations by the beginning of the MD era.

It is useful to Fourier transform over \vec{x} and integrate the fluctuations $F_1(\vec{x}, \vec{p}; t)$ over the momentum \vec{p} ,

$$\Delta(k, t) \equiv m \int \frac{d^3 p}{(2\pi)^3} F_1(\vec{k}, \vec{p}; t) \quad \text{where} \quad F_1(\vec{k}, \vec{p}; t) = \int d^3 x e^{-i \vec{x} \cdot \vec{k}} F_1(\vec{x}, \vec{p}; t). \quad (3.4)$$

Its Fourier transform provides the matter density fluctuations $\rho_{lin}(r)$ in linear approximation today

$$\rho_{lin}(r) = \frac{1}{2\pi^2 r} \int_0^\infty k dk \sin(kr) \Delta(k, t_{today}), \quad (3.5)$$

where as customary we considered a spherical symmetric distribution.

We therefore have as initial conditions using eqs.(3.3) and (3.4),

$$\Delta(k, t_{eq}) = \Omega_M \rho_c \delta(k, t_{eq}), \quad (3.6)$$

The present linear treatment is valid for small scales $k > k_{eq}$. Non-linear effects become important for large scales $k < k_{eq}$ and call for the use of the full (non-linear) Boltzmann-Vlasov equation or N -body simulations.

The density fluctuations $\delta(k, t)$ by the end of the radiation dominated (RD) era can be obtained analytically for subhorizon wavenumbers [15, 26]. The initial conditions for $\delta(k, t)$ in the RD era are the primordial inflationary fluctuations. With such initial conditions and solving the fluid equations for DM during the RD era yields [15, 26]

$$\delta(k, t_{eq}) = \frac{1}{2} A |\phi_k| \left\{ 5 \log \left[\frac{4\sqrt{2} B k}{k_{eq} (1 + \sqrt{2})^2} \right] + 6\sqrt{2} - 15 \right\} \sqrt{V} = \frac{5}{2} A |\phi_k| \log \left(0.2637 B \frac{k}{k_{eq}} \right) \sqrt{V}, \quad (3.7)$$

where $V = b_1/k_{eq}^3$ with $b_1 \sim 1$ is the comoving horizon volume by equilibration. Namely, all fluctuations with $k > k_{eq}$ that were inside the horizon by equilibration are relevant here. More explicitly, $k_{eq} \simeq 42.04 H_0 = 9.88 \text{ Gpc}^{-1}$ [15] and

$$\sqrt{V} \simeq \frac{b_1}{k_{eq}^{\frac{3}{2}}} \simeq \frac{b_1 b_0}{H_0^{\frac{3}{2}}} \quad \text{where} \quad b_0 \simeq 3.669 \cdot 10^{-3}. \quad (3.8)$$

$A \simeq 9.6$ and $B \simeq 0.44$ are constants that follow evolving the fluid equations [26], ϕ_k are the primordial inflationary fluctuations of the newtonian potential [9, 15]

$$|\phi_k| = \sqrt{2} \pi \frac{|\Delta_0|}{k^{\frac{3}{2}}} \left(\frac{k}{k_0} \right)^{\frac{n_s-1}{2}}, \quad (3.9)$$

$|\Delta_0|$ stands for the primordial power amplitude, n_s is the spectral index, and k_0 the pivot wavenumber [9, 27],

$$|\Delta_0| \simeq 4.94 \cdot 10^{-5}, \quad n_s \simeq 0.964, \quad k_0 = 2 \text{ Gpc}^{-1}. \quad (3.10)$$

It is convenient to define

$$\widehat{\Delta}(k, t) \equiv \frac{\Delta(k, t)}{\Delta(k, t_{eq})} \quad (3.11)$$

Then, the Gilbert equation takes the form [8]

$$\widehat{\Delta}(k, u) - \frac{6}{\alpha} \int_0^u \Pi[\alpha(u-u')] \frac{\widehat{\Delta}(k, u')}{[1-u']^2} du' = I[\alpha u], \quad (3.12)$$

where,

$$\begin{aligned} \Pi[z] &= \frac{1}{I_2} \int_0^\infty dy y f_0(y) \sin(yz) \quad , \quad I[z] = \frac{1}{I_2} \int_0^\infty dy y f_0(y) \frac{\sin(yz)}{z} \quad , \quad I_2 = \int_0^\infty dy y^2 f_0(y) \quad , \\ y &\equiv \frac{p}{T_d} \quad , \quad z \equiv \alpha u \quad , \quad \alpha \equiv \frac{2k}{H_0} \sqrt{\frac{1+z_{eq}}{\Omega_M}} \frac{T_d}{m} \quad , \quad 1+z_{eq} = \frac{1}{a_{eq}} \simeq 3200 \quad . \end{aligned} \quad (3.13)$$

u is a dimensionless time variable related to the scale factor by

$$u = 1 - \sqrt{\frac{a_{eq}}{a}} \quad , \quad a(u) = \frac{a_{eq}}{(1-u)^2} \quad ,$$

$$0 \leq u \leq u_{\text{today}} = 1 - \sqrt{a_{eq}} \simeq 0.982 \quad , \quad a(\text{today}) = 1 \quad .$$

It follows from the resolution of the Gilbert equation eq.(3.12) that for late times the solution grows as [8]

$$\widehat{\Delta}(k, t) \stackrel{t \rightarrow t_{\text{today}}}{\equiv} \frac{3}{5} T(k) (1+z_{eq}) \quad (3.14)$$

where $T(k)$ stands for the transfer function. That is, $\widehat{\Delta}(k, t)$ grows proportional to the scale factor in the linear approximation for all $k < k_{fs}$. The free-streaming comoving wavenumber k_{fs} increases with time as $1/\sqrt{1+z}$.

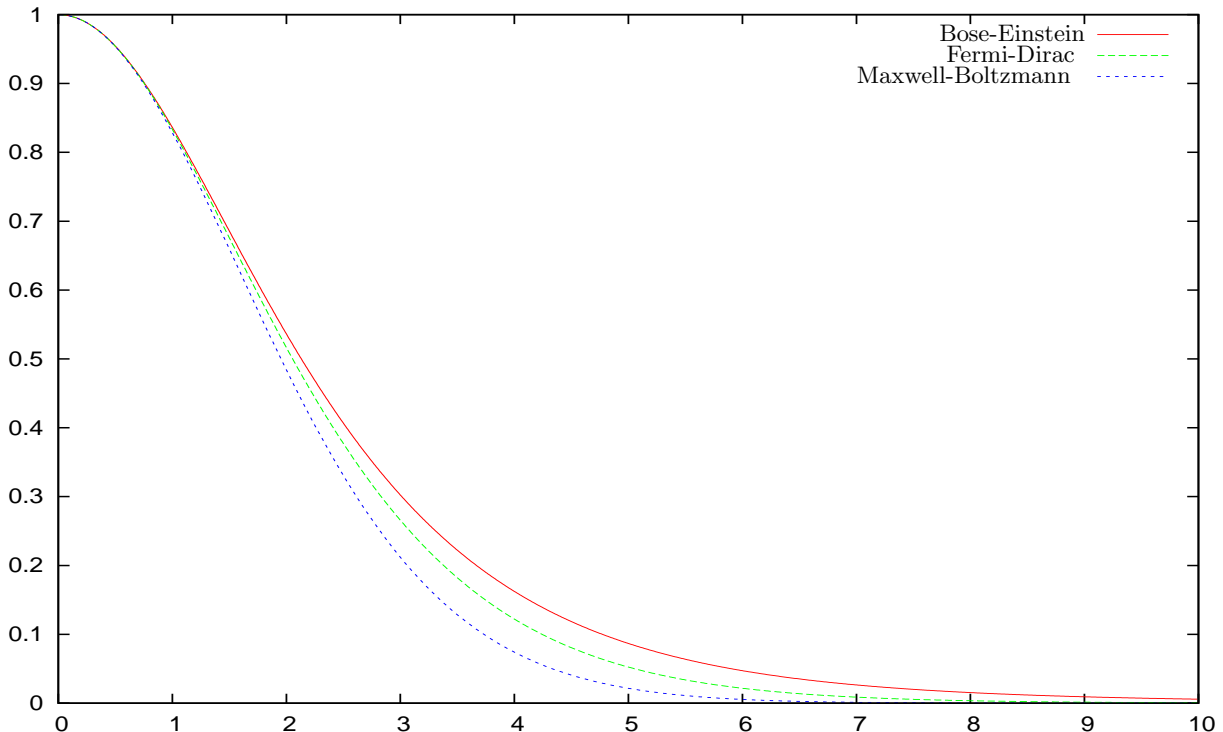


FIG. 1: The transfer function $T(k)$ vs. $\gamma = k r_{in}$ for Fermions and Bosons decoupling ultrarelativistically and for particles decoupling non-relativistically (Maxwell-Boltzmann statistics). We see that $T(k)$ decays for increasing k with a characteristic scale $\sim 1/r_{in} \sim k_{fs}$ [see eq.(3.17)].

$T(k)$ is obtained by solving the Gilbert equation (3.12) [8]. We plot in fig. 1 $T(k)$ for Fermions (FD) and Bosons (BE) decoupling ultrarelativistically and for particles decoupling non-relativistically (Maxwell-Boltzmann statistics,

MB). $T(k)$ enjoys the properties $T(0) = 1$ and $T(k \rightarrow \infty) = 0$. $T(k)$ decreases with k according to the characteristic scale given by the free streaming wavenumber k_{fs} where $l_{fs} = \sqrt{6}/k_{fs}$ is the free streaming length [8]. $T(k)$ shows little variation with the statistics of the DM particle. The explicit expression of the comoving free streaming length is

$$l_{fs} = \frac{2\sqrt{3}}{H_0} \sigma_{DM} \sqrt{\frac{1+z_{eq}}{\Omega_M}} \quad , \quad \sigma_{DM}^2 \equiv \frac{1}{3} \langle v^2 \rangle . \quad (3.15)$$

σ_{DM} stands for the primordial comoving squared velocity dispersion of the DM particles. That is, the velocity dispersion computed from the thermal equilibrium distribution function $f_0(p)$ which can be expressed as

$$\sigma_{DM} = \sqrt{\frac{I_4}{3I_2}} \frac{T_d}{m} \quad \text{where} \quad I_4 = \int_0^\infty dy y^4 f_0(y) . \quad (3.16)$$

It is convenient to introduce the dimensionless variable

$$\gamma \equiv k r_{lin} \quad \text{where} \quad r_{lin} \equiv \frac{l_{fs}}{\sqrt{3}} = \frac{\sqrt{2}}{k_{fs}} , \quad (3.17)$$

and consider the transfer function $T(k)$ as a function of γ . $T(\gamma)$ decreases by an amount of order one for γ increasing by unit. Therefore, its Fourier transform $\rho_{lin}(r)$ eq.(3.5), decreases with r having r_{lin} as characteristic scale.

The dark matter density eq.(3.1) can be also expressed as an integral over y [eq.(3.12)] as

$$\rho_{DM} = \frac{m}{2\pi^2} g T_d^3 I_2 . \quad (3.18)$$

The covariant decoupling temperature T_d can be related to the effective number of UR degrees of freedom at decoupling g_d and the photon temperature today T_{cmb} by using entropy conservation (see for example [6]):

$$T_d = \left(\frac{2}{g_d}\right)^{\frac{1}{3}} T_{cmb} , \quad \text{where} \quad T_{cmb} = 0.2348 \text{ meV} . \quad (3.19)$$

We obtain the amplitude $\Delta(k, t)$ today by inserting eqs. (3.6), (3.8), (3.7), (3.9) and (3.14) into eq.(3.11) for $t = t_{\text{today}}$ with the result:

$$\Delta(k, t_{\text{today}}) = \frac{9\pi}{\sqrt{2}} \frac{M_{Pl}^2}{H_0} \Omega_M b_0 b_1 A (1+z_{eq}) |\Delta_0| T(k) \left(\frac{k}{k_{eq}}\right)^{\frac{3}{2}} \left(\frac{k}{k_0}\right)^{\frac{n_s-1}{2}} \log\left(c \frac{k}{k_{eq}}\right) . \quad (3.20)$$

where $c = 0.11604$. Inserting eq.(3.20) into eq.(3.5) yields the density profile today,

$$\begin{aligned} \rho_{lin}(r) &= \frac{27\sqrt{2}}{5\pi} \frac{\Omega_M^2 M_{Pl}^2 H_0}{\sigma_{DM}^2} b_0 b_1 A |\Delta_0| (k_{eq} r_{lin})^{\frac{3}{2}} \frac{(k_0 r_{lin})^{\frac{1-n_s}{2}}}{r} \int_0^\infty d\gamma N(\gamma) \sin\left(\gamma \frac{r}{r_{lin}}\right) , \\ r_{lin} \rho_{lin}(0) &= \frac{27\sqrt{2}}{5\pi} \frac{\Omega_M^2 M_{Pl}^2 H_0}{\sigma_{DM}^2} b_0 b_1 A |\Delta_0| (k_{eq} r_{lin})^{\frac{3}{2}} (k_0 r_{lin})^{\frac{1-n_s}{2}} \int_0^\infty d\gamma \gamma N(\gamma) . \end{aligned} \quad (3.21)$$

where

$$N(\gamma) \equiv \gamma^{n_s/2-1} \log\left(\frac{c\gamma}{k_{eq} r_{lin}}\right) T(\gamma) .$$

Notice that there are no free parameters here. All parameters here are known cosmological parameters and the parameter Z determined by eq.(4.1).

From these results we compute and analyze the surface gravity and the density profile in the sections below.

IV. PROPERTIES OF THE LINEAR DENSITY PROFILE AND THE SURFACE GRAVITY

It is very useful to relate the free streaming length to the phase-space density ρ/σ^3 [7, 11, 13, 25]. ρ/σ^3 is invariant under the cosmological expansion and decreases due to gravitational clustering (self-gravity interactions). The phase-space density before structure formation (ρ_{DM}/σ_{DM}^3) and today can be related as [13]

$$\frac{\rho_s}{\sigma_s^3} = \frac{1}{Z} \frac{\rho_{DM}}{\sigma_{DM}^3} . \quad (4.1)$$

where ρ_{DM}/σ_{DM}^3 is the constant phase-space density before the MD era. The constant phase-space density today

$$\frac{\rho_s}{\sigma_s^3} \sim 5 \times 10^3 \frac{\text{keV}/\text{cm}^3}{(\text{km}/\text{s})^3} = (0.18 \text{ keV})^4, \quad (4.2)$$

follows from dSphs observations [48]. The range of values of the factor Z is discussed below and in sec. V.

We obtain the primordial DM dispersion velocity σ_{DM} from eqs. (3.1), (3.2) and (4.1) [13],

$$\sigma_{DM} = \left(3 M_{Pl}^2 H_0^2 \Omega_{DM} \frac{1}{Z} \frac{\sigma_s^3}{\rho_s} \right)^{\frac{1}{3}} \quad (4.3)$$

This expression is valid for **any kind** of DM particles. We find using eq.(3.15) for the free streaming length, eq.(4.3) for σ_{DM} , and eq.(4.2),

$$r_{lin} = \frac{l_{fs}}{\sqrt{3}} = \frac{207.6}{Z^{\frac{1}{3}}} \text{ kpc} = 96.37 \left(\frac{10}{Z} \right)^{\frac{1}{3}} \text{ kpc} \quad \text{and} \quad \frac{1}{\sigma_{DM}^2} = 2.358 \cdot 10^{13} Z^{\frac{2}{3}}. \quad (4.4)$$

The velocity dispersion $\sigma_{DM} \sim 10^{-7} Z^{-\frac{1}{3}} < 10^{-7}$ is very small since it does not take into account the self-gravity contrary to $\sigma_s \sim 10^{-5}$. σ_{DM} is just the covariant primordial velocity dispersion.

The linearized Boltzmann-Vlasov equation with the given initial conditions eqs.(3.6)-(3.7) provides a single solution that can be considered a galaxy configuration with characteristic size given by the linear scale r_{lin} which is of the order of the free-streaming length eq.(3.17) $r_{lin} \sim l_{fs}$. The length r_{lin} approaches the halo radius eq.(1.2) for the largest galaxies, $r_{lin} \gtrsim r_0$. Taking as initial conditions eq.(3.6) multiplied by a unit random gaussian field plus taking into account non-linear effects would give a variety of galaxy configurations with smaller masses and sizes.

Inserting eq.(4.4) r_{lin} and $1/\sigma_{DM}^2$, and the values eq.(3.10) in eq.(3.21) yields for the density profile and the surface gravity:

$$\rho_{lin}(r) = (5.826 \text{ Mev})^3 \frac{Z^{n_s/6}}{r} \int_0^\infty d\gamma N(\gamma) \sin\left(\gamma \frac{r}{r_{lin}}\right) \quad (4.5)$$

$$\mu_{0D} = r_{lin} \rho_{lin}(0) = (5.826 \text{ Mev})^3 Z^{n_s/6} \int_0^\infty d\gamma \gamma N(\gamma) \quad (4.6)$$

where $n_s/2 - 1 = -0.518$, $n_s/2 = 0.482$, $n_s/6 = 0.160$,

$$N(\gamma) \equiv \gamma^{n_s/2-1} \log\left(\hat{c} Z^{\frac{1}{3}} \gamma\right) T(\gamma),$$

and $\hat{c} = 43.6$.

Particle Statistics	$\mu_{0D} = r_{lin} \rho_{lin}(0)$	$r_{lin}^2 \rho_{lin}''(0)/\rho_{lin}(0)$
Bose-Einstein	$(16.71 \text{ Mev})^3 (Z/10)^{0.16}$	-5.50
Fermi-Dirac	$(15.65 \text{ Mev})^3 (Z/10)^{0.16}$	-2.74
Maxwell-Boltzmann	$(14.73 \text{ Mev})^3 (Z/10)^{0.16}$	-1.83

TABLE I: Values obtained of the surface gravity $\mu_{0D} = r_{lin} \rho_{lin}(0)$ for Fermions and Bosons decoupling ultrarelativistically and for particles decoupling non-relativistically (Maxwell-Boltzmann statistics). [The exponent of Z originates in the primordial power $n_s/6 = 0.16$]. The comparison of these theoretical results for $\mu_{0D} = r_{lin} \rho_{lin}(0)$ with the observational value eq.(1.1) indicates that $Z \sim 10 - 100$ and therefore that the DM particle mass is in the keV range [see eq.(5.4)]. In any case, the agreement between the linear theory and the observations is **remarkable**.

We plot in fig. 2 the ratio

$$\frac{\rho_{lin}(r)}{\rho_{lin}(0)} \equiv \Psi(x) = \frac{\int_0^\infty N(\gamma) \sin(\gamma x) d\gamma}{x \int_0^\infty \gamma N(\gamma) d\gamma}, \quad x \equiv r/r_{lin}, \quad (4.7)$$

for Fermions (FD) and Bosons (BE) decoupling ultrarelativistically and for particles decoupling non-relativistically [Maxwell-Boltzmann statistics (MB)]. Notice that $\Psi(x)$ is **independent** of the length scale r_{lin} . $\Psi(x)$ only depends on the cosmological parameters with a mild logarithmic dependence on Z , as shown by eqs.(4.5)-(4.6).

The theoretical results for μ_{0D} displayed in Table I confronted to the observed value eq.(1.1) suggest the values $Z \sim 10 - 100$. We choose for the plots a typical value $Z = 10$. However, the same picture is obtained for all

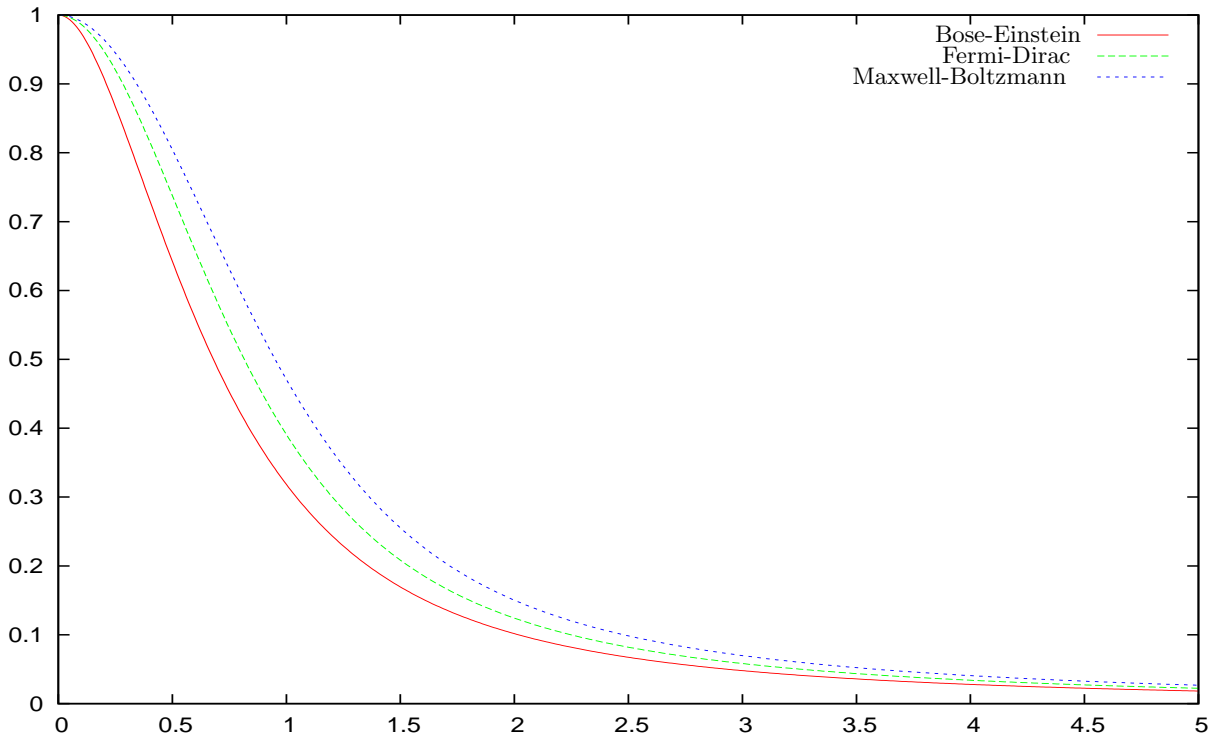


FIG. 2: The profiles $\rho_{lin}(r)/\rho_{lin}(0)$ vs. x , where $x \equiv r/r_{lin}$ for Fermions and Bosons decoupling ultrarelativistically and for particles decoupling non-relativistically (Maxwell-Boltzmann statistics). The bosons profile is the more peaked, the MB profile is the shallowest and the fermions profile is lying in-between.

$1 < Z < 10^4$ since the dependence on Z is mild. This is consistent with the independent analysis on the range of Z in [13].

The displayed profiles are clearly **cored**, as expected, since $T(k)$ decays for $k > k_{fs} \sim 1/r_{lin}$. Moreover, the profile eq.(4.5) is flat at $r = 0$ with a negative concavity there, namely $\rho'_{lin}(0) = 0$ and $\rho''_{lin}(0) < 0$. More explicitly,

$$\frac{\rho_{lin}(r)}{\rho_{lin}(0)} \stackrel{r \ll r_{lin}}{\approx} 1 + \frac{r^2}{2} \frac{\rho''_{lin}(0)}{\rho_{lin}(0)} + \mathcal{O}(r^4) = 1 - \frac{x^2}{6} \frac{\int_0^\infty \gamma^{2.482} \log\left(\hat{c} Z^{\frac{1}{3}} \gamma\right) T(\gamma) d\gamma}{\int_0^\infty \gamma^{0.482} \log\left(\hat{c} Z^{\frac{1}{3}} \gamma\right) T(\gamma) d\gamma} + \mathcal{O}(x^4).$$

We display in Table I the values of $r_{lin} \rho_{lin}(0)$ and $r_{lin}^2 \rho''_{lin}(0)/\rho_{lin}(0)$ for the three particle statistics: FD, BE and MB. We find that $\rho_{lin}(0)_{BE} > \rho_{lin}(0)_{FD} > \rho_{lin}(0)_{MB}$. We display in fig. 2 the profiles $\rho_{lin}(r)/\rho_{lin}(0)$ as functions of $x = r/r_{lin}$. The more peaked density profile is the one for bosons (BE) and the more shallow is the non-relativistic one (MB). The fermions profile being in-between the two other profiles.

V. CONCLUDING REMARKS AND THE DM PARTICLE MASS IN THE KEV SCALE

The astronomical observations tells us that the value of the surface gravity $\mu_{0D} = r_0 \rho(0)$ is **universal**. Therefore, we can compute μ_{0D} in the limiting case where the linearized Boltzmann-Vlasov equation holds. This is why we **identify** $r_{lin} \rho_{lin}(0)$ computed for a spherically symmetric solution of the linearized Boltzmann-Vlasov equation for self-gravitating DM with the **observed** value eqs.(1.1)-(1.2). One representative solution should be enough to obtain the value of the surface gravity but a more general treatment for non-spherically symmetrical solutions of the **non-linear** Boltzmann-Vlasov equation and/or N -body simulations (and including also baryonic matter) will be necessary to prove the universality of $r_0 \rho(0)$.

We can estimate the mass of the galaxies obtained in the linear approximation from eqs.(4.4)-(4.5) as

$$M \sim r_{lin}^3 \rho_{lin}(0) = 1.8 \cdot 10^{14} M_\odot \left(\frac{10}{Z}\right)^{\frac{4-n_s}{6}}, \quad \frac{4-n_s}{6} \simeq 0.506. \quad (5.1)$$

We obtain mass values in the upper range of the observations, as expected.

Notice the scaling of the linear profile $\rho_{lin}(r)$ eq.(4.5) obtained here with the primordial spectral index n_s : $\rho_{lin}(r)$ decreases as

$$r^{-1-n_s/2} = r^{-1.482} \quad \text{for } r \gg r_{lin} .$$

The value of this exponent is in agreement with the universal empirical behaviour recently put forward from observations in Walker et al. [47] and from Λ CDM simulations in Vass et al. [46]: $r^{-1.6 \pm 0.4}$. For larger scales we would expect that the contribution from small k modes where nonlinear effects are dominant will give the customary r^{-3} tail.

The range of values of Z from analytic approximate formulas both for linear fluctuations and the (non-linear) spherical model [13] and from N -body simulations results [24, 31, 33, 35, 36] is given by

$$1 < Z < 10000 .$$

We find that the surface gravity computed from the linearized Boltzmann-Vlasov equation reproduces very well the observed value of the energy scale eq.(1.1) for the three different particle statistics provided $Z \sim 10 - 100$ for dSphs. Nonlinear effects should improve the theoretical values of the surface gravity $\mu_{0D} = r_{lin} \rho_{lin}(0)$ in Table I including the contributions from large scales (small k modes). Notice from eq.(4.6) that the theoretically computed $\rho_{lin}(r)$ and μ_{0D} have a **mild** dependence on Z , the only parameter here which is not known with precision.

Anyhow, the agreement between the linear theory and the observations is already **remarkable**. The comparison of our theoretical values for μ_{0D} displayed in Table I and the observational value eq.(1.1) indicates that $Z \sim 10 - 100$ for dSphs.

Notice that r_{lin} in eq.(4.4) decreases with Z as $Z^{-\frac{1}{3}}$, while $\rho_{lin}(0)$ in eq.(4.6) grows with Z as $Z^{(n_s+2)/6} \ln Z = Z^{0.493} \ln Z$.

From Table I and eq.(4.4) we obtain for the density contrast between the galaxy center and the average DM density

$$\frac{\rho_{lin}(0)}{\rho_{DM}} \simeq 2 \times 10^4 \left(\frac{Z}{10} \right)^{\frac{n_s+2}{6}}$$

for FD particles and similar results for the BE and MB statistics. The value obtained here is smaller by about a factor ten than observations [38].

In summary, the solution of the linearized Boltzmann-Vlasov equation presented here provides an analytic and explicit approximative picture of a galaxy. Although nonlinear effects and baryons are not taken into account, this simple description qualitatively reproduces the main characteristics of a galaxy. Moreover, the agreement is even approximatively quantitative for r_{lin} eq.(4.4) with the observed halo radius. Similarly for M eq.(5.1) with the observed galaxy mass in the limiting case of large size galaxies.

Combining eqs.(3.16), (3.18), (3.19) and (4.1) we can express m and g_d as

$$m^4 = \frac{2 \pi^2}{3 \sqrt{3}} \frac{Z}{g} \frac{\rho_s}{\sigma_s^3} \frac{I_4^{\frac{3}{2}}}{I_2^{\frac{3}{2}}} , \quad m = 0.2504 \left(\frac{Z}{g} \right)^{\frac{1}{4}} \frac{I_4^{\frac{3}{8}}}{I_2^{\frac{3}{8}}} \text{ keV} , \quad (5.2)$$

$$g_d = \frac{2^{\frac{1}{4}}}{3^{\frac{11}{8}} \pi^{\frac{3}{2}}} \frac{g^{\frac{3}{4}}}{\Omega_{DM}} \frac{T_{cmb}^3}{M_{Pl}^2 H_0^2} \left(\frac{Z \rho_s}{\sigma_s^3} \right)^{\frac{1}{4}} (I_2 I_4)^{\frac{3}{8}} = 35.96 Z^{\frac{1}{4}} g^{\frac{3}{4}} (I_2 I_4)^{\frac{3}{8}} . \quad (5.3)$$

For example, for fermions and bosons that decouple ultrarelativistically at thermal equilibrium eqs.(5.2) and (5.3) yield [13]

$$m = \left(\frac{Z}{g} \right)^{\frac{1}{4}} \text{ keV} \times \begin{cases} 0.568 & \text{Fermions} \\ 0.484 & \text{Bosons} \end{cases} , \quad g_d = g^{\frac{3}{4}} Z^{\frac{1}{4}} \times \begin{cases} 155 & \text{Fermions} \\ 180 & \text{Bosons} \end{cases} . \quad (5.4)$$

Notice that $1 < Z^{\frac{1}{4}} < 10$ for $1 < Z < 10000$.

The range of values $1 < Z < 100$ discussed above and eqs.(5.2) and (5.4) imply that the DM particle mass is in the keV range.

The DM particle mass m grows as $Z^{\frac{1}{4}}$ according to eq.(5.2) (or as $Z^{\frac{1}{3}}$ for DM particles decoupling non-relativistically [13]). For example, wimps at $m = 100$ GeV and $T_d = 5$ GeV [12] would require $Z \sim 10^{24}$ [13]. For $Z \sim 10^{24}$ we find the characteristic scale r_{lin} eq.(4.4)

$$r_{lin} \sim 0.00208 \text{ pc} \sim 438 \text{ AU}$$

For such **small** r_{lin} the linear profile $\rho_{lin}(r)$ would appear as a **cusped** profile when observed at scales of the kpc or larger as eq.(4.7) and fig. 2 show. Cusped profiles are thus clearly associated to heavy DM particles with a huge mass

m well above the physical keV scale. Wimps with $Z \sim 10^{24}$ are in contradiction with the observed value eq.(1.1) of the surface gravity as shown by Table I.

Independent further evidence for the DM particle mass in the keV scale were recently given in Song & Lee [40], Tikhonov et al. [43]. (See also Wyse & Gilmore [48]). DM particles with mass in the keV scale can alleviate CDM problems as the satellite problem [39] and the voids problem [45].

The DM particle mass in the keV scale explain why DM particles were not found in detectors sensitive to particles heavier than ~ 1 GeV [1]. In addition, astrophysical mechanisms that can explain the e^+ and \bar{p} excess in cosmic rays without requiring DM particles in the GeV scale or above were put forward in Biermann, et al. [2], Blasi [3], Blasi & Serpico [4].

Our present results for the surface gravity and the density profile, besides their intrinsic interest giving clues to explain the universal value of the surface gravity, provide further evidence for the mass scale of the DM particle being in the keV scale.

Acknowledgments

We thank Claudio Destri and Paolo Salucci for useful discussions.

-
- [1] Z. Ahmed et al., arXiv:0912.3592.
[2] P.L. Biermann, et al., PRL 103:061101 (2009).
[3] P. Blasi, PRL 103:051104 (2009).
[4] P. Blasi, P. D. Serpico, PRL 103:081103 (2009).
[5] J. R. Bond, A. S. Szalay, Astrophys. J. **274**, 443 (1983).
[6] G. Börner, *The Early Universe*, Springer, 2003.
[7] D. Boyanovsky, H J de Vega, N. G. Sanchez, Phys. Rev. **D 77**, 043518 (2008).
[8] D. Boyanovsky, H J de Vega, N. G. Sanchez, Phys. Rev. **D 78**, 063546 (2008).
[9] D. Boyanovsky, C. Destri, H. J. de Vega, N. G. Sánchez, arXiv:0901.0549, Int. J. Mod. Phys. **A 24**, 3669-3864 (2009).
[10] A. Burkert, ApJ, 447, L25 (1995).
[11] J. J. Dalcanton, C. J. Hogan, Astrophys. J. **561**, 35 (2001).
[12] See, for example, Dark Matter in <http://pdg.lbl.gov/2009/reviews/>
[13] H J de Vega, N. G. Sanchez, arXiv:0901.0922, Mon. Not. R. Astron. Soc. 404, 885 (2010).
[14] M J Disney et al. Nature 455, 1082 (2008), arXiv:0811.1554.
[15] Dodelson S, *Modern Cosmology*, Academic Press, 2003.
[16] F. Donato et al., MNRAS **397**, 1169 (2009).
[17] D. A. Garcia-Appadoo et al., Mon. Not. Roy. Astron. Soc. 394:340, (2009).
[18] G Gentile et al., Nature, 461, 627 (2009).
[19] I. H. Gilbert, Astrophys. J. **144**, 233 (1966); *ibid*, **152**, 1043 (1968).
[20] G. Gilmore *et. al.* Astrophys. J, 663, 948 (2007).
[21] G. Gilmore, arXiv:0808.3188.
[22] P. F. Goldsmith et al. ApJ, 680, 428 (2008) and references therein.
[23] M. Heyer et al. ApJ, 699, 1092 (2009).
[24] Y. Hoffman *et.al.* Astrophys. J. **671**, 1108 (2007).
[25] C. J. Hogan, J. J. Dalcanton, Phys. Rev. **D62**, 063511 (2000).
[26] W. Hu, N. Sugiyama, Astrophys. J. **471**, 542 (1996).
[27] E. Komatsu et al. (WMAP collaboration), Astrophys. J. Suppl. 180:330 (2009).
[28] J Kormendy, K C Freeman, IAU Symposium, Sydney, 220, 377 (2004), arXiv:astro-ph/0407321.
[29] L. D. Landau, E. M. Lifshitz, Mechanics, Pergamon Press, London, 1960.
[30] L. D. Landau, E. M. Lifshitz, Statistical Physics, Reed Elsevier, Oxford, 1980.
[31] A. Lapi, A. Cavaliere, Astrophys. J. **692**, 1, 174 (2009).
[32] R. B. Larson, MNRAS, 194, 809 (1981).
[33] S. Peirani *et. al.*, Mon. Not. R. Astron. Soc. **367**, 1011 (2006).
[34] M. Persic, P. Salucci, F. Stel, MNRAS, 281, 27 (1996).
[35] E. Romano-Diaz *et.al.*, Astrophys. J. **637**, L93 (2006).
[36] E. Romano-Diaz *et.al.*, Astrophys. J. **657**, 56 (2007).
[37] E. Rosolowsky and L. Blitz, ApJ 623, 826 (2005).
[38] P. Salucci, M. Persic, ASP Proceedings 1997, astro-ph/9703027.
[39] J. Sommer-Larsen, A. Dolgov, ApJ, 551, 608 (2001).
[40] H. S. Song, J. Lee, ApJL 703, L14 (2009).
[41] M. Spano et al., MNRAS, 383, 297 (2008).
[42] L. E. Strigari et al., Nature, 454, 1096 (2008).
[43] A. V. Tikhonov et al. Mon. Not. R. Astron. Soc. **399**, 1611 (2009).
[44] S van den Bergh, arXiv:0810.3644, Nature 455, 1049 (2008).

- [45] R. van de Weygaert, E. Platen, COSPA2008 review, arXiv:0912.2997.
- [46] I. M. Vass et al., *Mon. Not. R. Astron. Soc.* **395**, 1225 (2009).
- [47] M. G. Walker et al., *ApJ*, 704, 1274 (2009).
- [48] R. F. G. Wyse and G. Gilmore, arXiv:0708.1492.